# Online Resource 1 Supplementary methods and results

Manuscript: Small roped closures held more harvestable *Cyclina sinensis* biomass in a Taiwanese wetland open to public clam digging

Journal: Wetlands Ecology and Management

Ching-Sung G. Chang[a,*], Jia-Siang Jhao[b], Ahmed Salah-Tantawy[b,c], Shuh-Sen Young[b]

[a] Institute of Bioinformatics and Systems Biology, National Yang Ming Chiao Tung University, Hsinchu City, 300, Taiwan

[b] Institute of Analytical and Environmental Sciences, National Tsing Hua University, Hsinchu City, 300, Taiwan

[c] Marine Science Division, Department of Zoology, College of Science, Al-Azhar University, Assiut, 71524, Egypt

Corresponding author: Ching-Sung G. Chang; cschang.bt10@nycu.edu.tw

ORCID: Ching-Sung G. Chang, https://orcid.org/0009-0002-0351-5934

ORCID: Ahmed Salah-Tantawy, https://orcid.org/0000-0003-4467-9054

## Supplementary methods

### Data provenance and completeness

The complete December and June datasets formed the principal treatment comparisons. The study comprised 16 stations, with 6 $m^2$ per plot. We excluded other station labels and confirmed zero catches where complete sampled catches had no entries. August HS2 remained unresolved, so monthly context and growth reconstruction used the same 15 stations, excluding HS2. Most April 2021 records had been lost; that month was omitted. January–March and May lacked complete weights. U denotes the unfenced treatment throughout the manuscript and supplementary data; C1 and C2 denote the two closure histories. C1 and C2 stayed fixed at the center of each station's sampling layout, while monthly U samples used different previously unexcavated positions around them. The *C. sinensis* collection protocol was 6 $m^2$, approximately 10-cm excavation and visual collection without a sieve in every month and treatment.

Maximum shell length was recorded in the original Width field for *C. sinensis*. We corrected two June entries to 14.3 and 14.5 mm and resolved one conflicting treatment assignment as C1. Original measurements were preserved. Corrections are listed in corrections.csv (Online Resource 2). The two length corrections leave those animals below the 30-mm threshold.

Treatment models use 16 stations. The monthly figure uses the same 15 stations for its unfenced and closure observations. Arithmetic-mean intervals resample stations and are pointwise rather than simultaneous intervals.

Online Resource 2 (ESM_2.zip) provides twenty-six CSV tables and a primary-model reproduction script, with a README and metadata inventory identifying the companion manuscript. The inputs include 80 station-treatment-date plots and 1,147 corrected individual measurements for the primary comparisons. All treatment labels and configuration prefixes use U for unfenced plots. CSVs use UTF-8 without a byte-order mark; the data dictionary defines the new input fields, units and confirmed-zero flag.

**Full endpoint models and sensitivity checks**

Complete effects are in Table S1. Harvestable and total mass use log-link Tweedie models; counts use log-link negative-binomial models, with a log-area offset and station intercept. Grouped counts above and at or below 30 mm use beta-binomial models on nonempty plots. Two December negative-binomial fits, at 26 and 26.28 mm, reached a dispersion boundary and failed Hessian checks; valid Poisson-limit fits replace them for inference. Failed fits remain in the diagnostic table. Three closure/U probabilities were Holm-adjusted separately within each endpoint family. Unadjusted Wald effect intervals are distinguished from adjusted probabilities.

Station-bootstrap comparisons are in Table S2. The station bootstrap retained each sampled station's full treatment vector. There were 2,000 draws, seed 20261103. Ratios of summed catch or mass are reported with percentile intervals. This ratio-of-totals target differs from the conditional model ratio. Primary paired Wilcoxon tests used the normal approximation, continuity correction and omission of zero differences. The three primary comparisons had adjusted $p = 0.0176$. Plot-level inputs and corrected individual measurements are provided in plot_level_data.csv and individual_measurements.csv in Online Resource 2.

The two-date model included treatment, date and their interaction with station and station-by-date intercepts. The C1/U biomass ratio of ratios was 1.069, with 95% interval 0.426–2.682. This describes compatibility between the observed contrasts. Size distributions were summarized by pooled quantiles with station-resampling intervals; individual-level KS tests were descriptive. Raw range was excluded as an inferential measure. Densities above the two Korean maturity-reference lengths retain their status as threshold proxies rather than measurements of local reproductive output.

**Exploratory growth inputs and settings**

Core parameter sensitivity is summarized in Table S3. The length-frequency input comprised 1,075 U animals from 15 common stations over 13 count-complete months. April and HS2 were excluded. Adding closure measurements in December and June was a separate sensitivity analysis. Bin widths 1, 2, 2.5 and 3 mm were crossed with moving-average widths 3, 5 and 7. Each core setting used 200 within-month case resamples, preserving monthly sample totals, rather than resampling stations. Restructuring and curve scoring followed TropFishR and fishboot functionality (Mildenberger et al. 2017; Taylor and Mildenberger 2017; Schwamborn et al. 2019). No component was assigned to a biological age class.

Core search bounds were $L_\infty$ 50.0616–80 mm, $K$ 0.1–1.5 $yr^{-1}$ and $t_{anchor}$ 0–1. The lower $L_\infty$ bound was 1.02 times the observed maximum 49.08 mm. A stress analysis extended $L_\infty$ to 100 mm and $K$ to 0.02–2 $yr^{-1}$. Initial values were 60 mm, 0.35 $yr^{-1}$ and 0.5. The principal bootstrap optimizer budget was 4 seconds, maximum 120 iterations and initial temperature 200,000. The 20-year curve horizon was a computational setting rather than an inferred lifespan. Longer unresampled checks used four optimizer seeds, with 8-second screens and 30-second reporting-setting checks. R 4.6.1, TropFishR 1.6.6, fishboot 1.0.4 and GenSA 1.1.15 were used. A local function copy explicitly passed negative optimizer seeds to GenSA, retaining the installed packages unchanged. The driver seed was 20261104 plus replicate index; the GenSA seed was its negative.

The reporting setting of 2 mm/MA5 was chosen as an intermediate bin width before inspecting the complete bootstrap summaries. Pooling and stress sensitivities used 200 resamples each; earlier/later date sensitivities used 50 each, for 2,900 bootstrap fits in total. There were 64 unresampled optimizer checks. For September 2020, December 2020 and June 2021 only the sampling month was known: the 15th was used in the main input, with the 1st and 28th as date sensitivities. Exact recorded days were retained for the remaining dates. These assumptions are documented and remain separate from observed dates.

**Calendar time and the curve anchor**

All saved fitted curves are nonseasonal. No fitted seasonal amplitude $C$ or seasonal phase $t_s$ is available, and no new seasonal search was undertaken for this manuscript. $K$ has units $yr^{-1}$, with years representing elapsed calendar time. A nonseasonal von Bertalanffy curve smooths over seasonal variation; its instantaneous length increment still depends on current size and decreases as length approaches $L_\infty$. It therefore does not assume a constant number of millimeters of growth each day. Start-month differences in realized growth remain unestimated.

In TropFishR, $t_{anchor}$ locates the annual repetition of a curve's extrapolated zero-length crossing in calendar coordinates (Mildenberger et al. 2017). It aligns curves to the sampled time axis. It is not an observed birth, settlement or first growth-ring date, and it does not identify the local biological age origin. The growth outputs are expressed as parameter sensitivity and time between specified lengths. A comparison with biological-age categories would require an independent match between the literature age definition and the model origin.

For two lengths on a nonseasonal fitted curve, the elapsed interval is

$$\Delta t = \frac{ln\left[\frac{L_\infty - L_{start}}{L_\infty - L_{target}}\right]}{K}$$

Multiplication by 12 converts years to months. The age-origin parameter cancels. Reported intervals are average calendar-time scenarios along the fitted curve, not season-specific forecasts or minimum closure durations. Fig. S1 summarizes the

length-to-length scenarios. Median times from 10 to 30 mm span 17.89–54.44 months among the 12 core settings. The minimum saved bootstrap interval is 3.93 months at 2 mm/MA7. The corresponding curve is outside an exploratory family-reference band but is retained in the unfiltered ensemble. Even the separate band-compatible subset has a minimum 8.31 months. Minima of finite saved ensembles and percentile ranges do not establish physical limits or demographic probabilities.

**Comparisons anchored to measured shell lengths**

Table S4 compares dated lengths without matching biological age to the model origin. Yu et al. (1996), pp 34–36, used shell growth rings and translucent bands for some age assignments and also reported dated stocking observations. The paper gives no independently established calendar date for formation of the first ring. Ring categories therefore remain distinct from elapsed years following birth or settlement. Table 1 provides initial lengths 29.6, 25.9 and 23.2 mm in July 1987 and subsequent lengths 39.3, 36.2 and 36.5 mm in August 1988. The authors describe approximately one annual cycle; the month labels span about 13 calendar months. Exact days are unavailable. The lower-flat comparison in Table 2 increased from 25.9 to 42.2 mm across the same labeled months. The higher-flat 25.9 to 36.2-mm group duplicates a Table 1 group and is not counted as an independent additional observation.

We compared each observed interval with existing fitted curves starting at its measured initial length. For each setting, we calculated predicted length after 12 calendar months, predicted length over the nominal 13-month source interval and conditional time to the reported endpoint. These are length-anchored descriptions with an explicit time convention. Differences among culture environments, repeated samples and individual trajectories remain relevant, so the comparison is contextual rather than a calibration test. No birth-date or first-ring assumption enters the calculation.

Feng et al. (2003), pp 92–94, describe a culture sequence beginning with April stocking. Mean stocking length was 25 mm; the first April sample mean was 26.1 mm and the following October mean 38 mm. The authors describe an 18-month culture period. The latter date marks the size comparison; harvest is described for November. We retained 25 and 26.1 mm as separate starts, comparing the fitted 18-month increments and times to 38 mm. These observations came from repeated random samples, not tracked individuals or known settlement dates. Feng fitted power/polynomial curves and a length–weight relationship, and Yu reported allometry and growth observations; neither paper reports a VBGF $L_\infty$–$K$ fit. Their original time definitions are retained rather than recast as biological ages.

**Interpreting sensitivity**

The median $K$ range across core settings is 2.51-fold. Boundary fits and occasional retention of the optimizer's initial point also occur. The saved budgets therefore leave both optimization and information limitations relevant. Growth-performance indices were standardized to centimeters and years before comparison with independent venerid studies (Goshima et al.

1996; Sienes et al. 2022; Mahé et al. 2024). The reference interval was used for flags and separately labeled summaries, not for deleting curves. Cross-species values and external observations do not supply local age validation. The primary closure findings are based on observed station stocks and remain independent of this exploratory reconstruction.

**Limited non-target density comparison**

June *Parilaternula certa* catches totaled 1,136 in C1, 1,178 in C2 and 1,230 in U over 96 $m^2$ per treatment, giving 11.83, 12.27 and 12.81 individuals $m^{-2}$, respectively. Table S5 reports the density contrasts and paired checks. The negative-binomial log-link model included species, treatment and their interaction, a station intercept, a log-area offset and species-specific dispersion. It converged with a positive-definite Hessian. Density ratios for C1/U, C2/U and C1/C2 were 0.99 (95% CI 0.23–4.19), 0.96 (0.23–4.06) and 1.03 (0.25–4.33), with unadjusted Wald $p$ = 0.988, 0.954 and 0.966. Paired Wilcoxon $p$ values were 0.724, 0.724 and 0.824. These wide intervals provide no evidence of a density contrast but do not establish equivalence or a different response from *C. sinensis*. December *P. certa* catches were confirmed zero and were not modeled.

**Prospective monitoring simulations**

Fig. S2 shows prospective power. Simulations used paired 6-$m^2$ unfenced and closure plots at 8, 16, 24, 32 and 48 stations. True mass ratios were 1, 1.5, 2 and 3, with 500 simulations per scenario. June primary-model nuisance values were intercept 0.6895065 on the log-density scale, station standard deviation 0.6147618, Tweedie dispersion 10.94089 and power 1.234560. Replicate seeds followed 20261105 +10000×scenario +replicate. Each dataset was refitted; failed fits counted as non-rejections. Additional scenarios multiplied dispersion by 0.75 or 1.5.

Nominal 5% Wald testing showed simulated null rejection rates of 0.082, 0.068, 0.056, 0.058 and 0.056 across increasing station numbers. We therefore also used the empirical 5% null cutoff for each station number to summarize calibrated power. Monte Carlo sensitivity intervals combined binomial bounds with resampling of the calibration and alternative simulations. The calibration resampling used seed 20261106. Field variance components were held fixed, so these intervals concern simulation uncertainty rather than all uncertainty in future environmental variation. For a twofold ratio, calibrated power at 16, 24, 32 and 48 stations was 0.418, 0.616, 0.772 and 0.852, respectively.

## Supplementary references

Feng MS, Sun XW, Gao SL (2003) Growth and development of cultured *Cyclina sinensis* (in Chinese). Chinese Agricultural Science Bulletin 19(2):92–94.

144 Goshima S, Ide N, Fujiyoshi Y, Noda T, Nakao S (1996) Reproductive cycle and shell growth of transplanted Manila clam
145 *Ruditapes philippinarum* in Saroma Lagoon. Nippon Suisan Gakkaishi 62(2):195–200.
146 https://doi.org/10.2331/suisan.62.195

147 Mahé M, Camus L, Marschal C, Grisel R, Poggiale JC, Mayot N (2024) Population dynamics of *Ruditapes philippinarum*
148 (A. Adams & Reeve, 1850) after the major ecological crisis of 2018 of the Berre lagoon, southern France. Journal of
149 Molluscan Studies 90(2):eyae009. https://doi.org/10.1093/mollus/eyae009

150 Mildenberger TK, Taylor MH, Wolff M (2017) TropFishR: an R package for fisheries analysis with length-frequency data.
151 Methods in Ecology and Evolution 8:1520–1527. https://doi.org/10.1111/2041-210X.12791

152 Schwamborn R, Mildenberger TK, Taylor MH (2019) Assessing sources of uncertainty in length-based estimates of body
153 growth in populations of fishes and macroinvertebrates with bootstrapped ELEFAN. Ecological Modelling 393:37–51.
154 https://doi.org/10.1016/j.ecolmodel.2018.12.001

155 Sienes RKA, Lucaser MAO, Metillo EB (2022) Population parameters of Asiatic hard clam, *Meretrix meretrix* (Bivalvia:
156 Veneridae), in Panguil Bay, Philippines. Mindanao Journal of Science and Technology 20(2):228–242.

157 Taylor MH, Mildenberger TK (2017) Extending electronic length frequency analysis in R. Fisheries Management and
158 Ecology 24:330–338. https://doi.org/10.1111/fme.12232

159 Yu YS, Wang H, Huang ZP, Lu P, Wu JX (1996) A preliminary study on the growth of *Cyclina sinensis* (in Chinese).
160 Chinese Journal of Zoology 31(4):34–36.

**Table S1** Valid model effects for closure versus unfenced plots

| Comparison | Endpoint | Ratio or odds ratio | 95% interval | Holm p |
|---|---|---|---|---|
| 2020-12 C1/U | Harvestable mass | 3.25 | 1.60–6.60 | 0.0019 |
| 2020-12 C1/U | Total density | 2.86 | 2.09–3.93 | <0.0001 |
| 2020-12 C1/U | Total mass | 2.86 | 1.92–4.25 | <0.0001 |
| 2020-12 C1/U | Density >30 mm | 2.78 | 1.42–5.45 | 0.0028 |
| 2020-12 C1/U | Large fraction odds | 1.26 | 0.57–2.78 | 0.783 |
| 2020-12 C1/U | Density >26 mm | 2.48 | 1.73–3.54 | <0.0001 |
| 2020-12 C1/U | Density >26.28 mm | 2.39 | 1.66–3.44 | <0.0001 |
| 2020-12 C1/U | Density >26.85 mm | 2.59 | 1.74–3.84 | <0.0001 |
| 2020-12 C1/U | Density >27 mm | 2.81 | 1.86–4.23 | <0.0001 |
| 2021-06 C1/U | Harvestable mass | 3.55 | 1.76–7.16 | 0.0012 |
| 2021-06 C2/U | Harvestable mass | 3.30 | 1.63–6.70 | 0.0019 |
| 2021-06 C1/U | Total density | 2.88 | 1.68–4.95 | 0.0003 |
| 2021-06 C2/U | Total density | 2.02 | 1.16–3.50 | 0.0126 |
| 2021-06 C1/U | Total mass | 2.77 | 1.70–4.52 | <0.0001 |
| 2021-06 C2/U | Total mass | 2.37 | 1.44–3.91 | 0.0007 |
| 2021-06 C1/U | Density >30 mm | 3.76 | 1.84–7.68 | 0.0008 |
| 2021-06 C2/U | Density >30 mm | 3.49 | 1.70–7.16 | 0.0013 |
| 2021-06 C1/U | Large fraction odds | 1.49 | 0.60–3.68 | 0.783 |
| 2021-06 C2/U | Large fraction odds | 1.98 | 0.79–4.95 | 0.431 |
| 2021-06 C1/U | Density >26 mm | 2.64 | 1.49–4.66 | 0.0016 |
| 2021-06 C2/U | Density >26 mm | 2.18 | 1.21–3.92 | 0.0097 |
| 2021-06 C1/U | Density >26.28 mm | 2.62 | 1.48–4.66 | 0.0020 |
| 2021-06 C2/U | Density >26.28 mm | 2.16 | 1.19–3.92 | 0.0111 |
| 2021-06 C1/U | Density >26.85 mm | 2.45 | 1.40–4.27 | 0.0033 |
| 2021-06 C2/U | Density >26.85 mm | 2.09 | 1.18–3.72 | 0.0117 |
| 2021-06 C1/U | Density >27 mm | 2.76 | 1.56–4.86 | 0.0009 |
| 2021-06 C2/U | Density >27 mm | 2.32 | 1.29–4.17 | 0.0048 |

Intervals are unadjusted Wald intervals. Holm adjustment is applied separately within each endpoint. The December >26 and >26.28-mm entries use valid Poisson-limit fits; failed negative-binomial versions remain in endpoint_model_diagnostics.csv.

**Table S2** Station bootstrap stock ratios

| Comparison | Endpoint | Ratio of totals | 95% percentile interval |
|---|---|---|---|
| 2020-12 C1/U | Harvestable mass | 3.38 | 1.62–6.60 |
| 2021-06 C1/U | Harvestable mass | 3.39 | 1.68–10.13 |
| 2021-06 C2/U | Harvestable mass | 3.08 | 1.53–11.78 |
| Jun C1 / Dec C1 | Total density | 1.52 | 0.95–2.49 |
| Jun C1 / Dec C1 | Harvestable mass | 0.93 | 0.46–2.24 |
| Jun C1 / Jun C2 | Total density | 1.36 | 0.81–2.26 |
| Jun C1 / Jun C2 | Harvestable mass | 1.10 | 0.56–2.19 |

**Table S3** Core nonseasonal growth sensitivity

| Bin (mm) | MA | $K$ ($yr^{-1}$) median (range) | $L_\infty$ (mm) median (range) | $\varphi'$ median | Near boundary (%) |
|---|---|---|---|---|---|
| 1 | 3 | 0.123 (0.100–0.223) | 55.20 (50.35–70.75) | 0.596 | 61.5 |
| 1 | 5 | 0.123 (0.102–0.231) | 54.52 (50.37–77.72) | 0.610 | 60.0 |
| 1 | 7 | 0.131 (0.101–0.356) | 56.98 (50.40–73.62) | 0.646 | 50.5 |
| 2 | 3 | 0.134 (0.101–0.259) | 56.02 (50.35–73.91) | 0.652 | 48.5 |
| 2 | 5 | 0.145 (0.102–0.383) | 56.47 (50.25–77.31) | 0.699 | 44.0 |
| 2 | 7 | 0.178 (0.101–0.389) | 58.12 (50.23–78.55) | 0.845 | 36.0 |
| 2.5 | 3 | 0.145 (0.102–0.316) | 57.06 (50.40–75.16) | 0.721 | 41.5 |
| 2.5 | 5 | 0.178 (0.103–0.439) | 58.68 (50.25–78.31) | 0.851 | 32.0 |
| 2.5 | 7 | 0.205 (0.100–0.577) | 57.06 (50.40–77.67) | 0.966 | 40.5 |
| 3 | 3 | 0.208 (0.106–0.411) | 59.12 (50.36–78.38) | 0.891 | 20.5 |
| 3 | 5 | 0.280 (0.127–0.406) | 60.00 (51.49–77.95) | 1.034 | 3.5 |
| 3 | 7 | 0.308 (0.104–0.470) | 60.00 (50.73–79.06) | 1.100 | 15.5 |

Ranges are the 2.5–97.5 percentiles of 200 case-bootstrap fits per setting. The near-boundary flag uses a 2% fraction of either declared $L_\infty/K$ search range. $\varphi'$ uses centimeters and years. These are sensitivity distributions under the recorded optimizer budgets

**Table S4** Length anchored external comparisons at 2 mm and MA5

| Source group | Start to end (mm) | Nominal months | Predicted end mm median (range) | Time to end months median (range) |
|---|---|---|---|---|
| Yu Table1 A | 29.6 to 39.3 | 13 | 33.8 (31.9–38.6) | 33.7 (14.2–68.4) |
| Yu Table1 B | 25.9 to 36.2 | 13 | 30.7 (28.7–35.9) | 31.6 (13.4–59.5) |
| Yu Table1 C | 23.2 to 36.5 | 13 | 28.4 (26.3–33.9) | 39.3 (16.9–73.2) |
| Yu Table2 lower flat | 25.9 to 42.2 | 13 | 30.7 (28.7–35.9) | 57.1 (23.9–118.5) |
| Feng stocking mean | 25.0 to 38.0 | 18 | 31.6 (28.9–38.6) | 41.0 (17.1–78.2) |
| Feng first April mean | 26.1 to 38.0 | 18 | 32.4 (29.8–39.1) | 38.1 (15.8–73.4) |

Monthly dates imply approximately 13 months for Yu July1987–August1988, although the text describes an annual cycle. Feng compares April with the next October, approximately 18 months. Ranges are bootstrap percentiles, with no assumption about birth date or ring age. All settings and 12-month predictions are provided in external_length_anchored_comparisons.csv.

**Table S5** June non-target *Parilaternula certa* density comparisons

| Comparison | Density ratio | 95% interval | Wald p | Paired-rank p |
|---|---|---|---|---|
| C1/U | 0.99 | 0.23–4.19 | 0.988 | 0.724 |
| C2/U | 0.96 | 0.23–4.06 | 0.954 | 0.724 |
| C1/C2 | 1.03 | 0.25–4.33 | 0.966 | 0.824 |

All intervals and probabilities are unadjusted. The count model uses species-by-treatment effects, species-specific dispersion, a station intercept and an area offset; paired-rank tests use the normal approximation with continuity correction. Complete density counts and source results are in Online Resource 2.

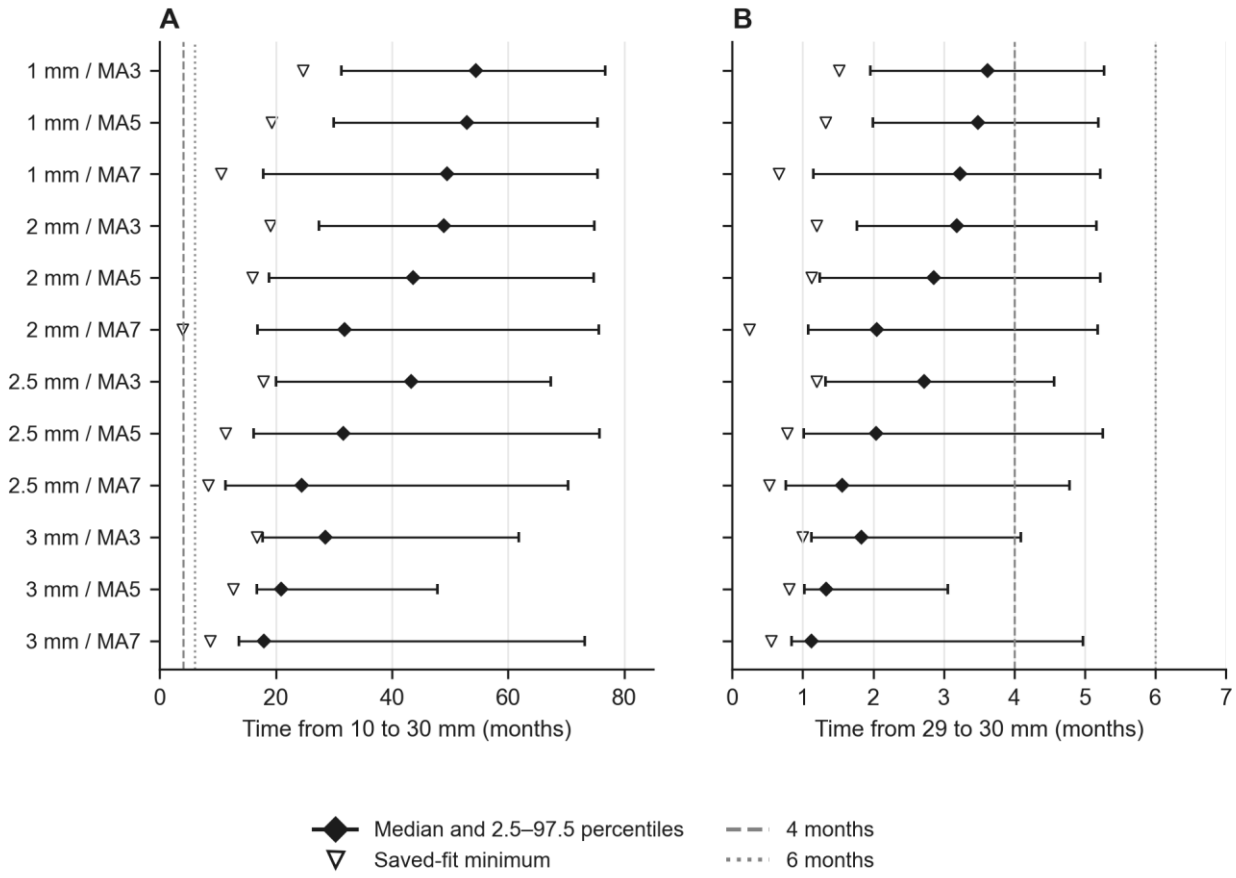
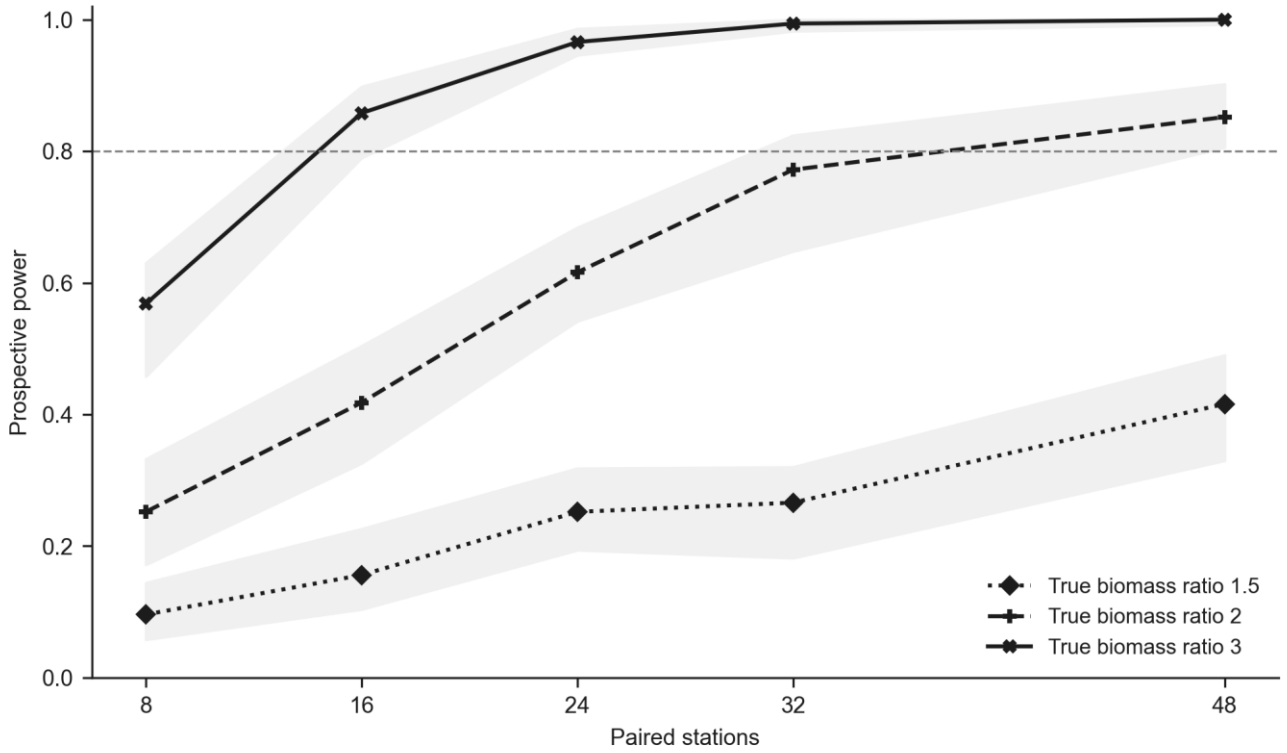



**Fig. S1** Nonseasonal average-calendar-time increments across the twelve core settings, from (A) 10 to 30 mm and (B) 29 to 30 mm. Filled diamonds and bars show medians and 2.5–97.5 percentiles, open downward triangles minima among saved fits. Dashed and dotted lines indicate four and six months. Panel scales differ; these summaries are not validated biological time limits




184

185 **Fig. S2** Prospective monitoring sensitivity after empirical null calibration. Simulations use the fitted June variation.
186 Shading indicates Monte Carlo sensitivity including null-calibration resampling, while nuisance values remain fixed